

Inhibitory control of neostriatal projection neurons by GABAergic interneurons

Tibor Koós and James M. Tepper

Center for Molecular and Behavioral Neuroscience and Program in Cellular and Molecular Biodynamics, Rutgers, The State University of New Jersey, 197 University Ave, Newark, New Jersey 07102, USA

Correspondence should be addressed to J.M.T. (tepper@axon.rutgers.edu)

The basal ganglia are a highly interconnected network of nuclei essential for the modulation and execution of voluntary behavior. The neostriatum is the principal input and one of the principal controllers of the output of the basal ganglia. Neostriatal projection neurons seem to be dynamically and powerfully controlled by GABAergic inputs, but the source(s) and physiological properties of these inputs remain unclear. Here we use paired whole-cell recordings to show that this inhibition derives from small populations of GABAergic interneurons that are themselves interconnected through functional electrotonic synapses. Inhibitory synaptic potentials generated from single interneurons are sufficiently powerful to delay or entirely block the generation of action potentials in a large number of projection neurons simultaneously.

The neostriatum is critically involved in the control and execution of voluntary behavior. Malfunctions of this system underlie several neurological and psychiatric disorders, including Parkinson's disease and Huntington's disease. Understanding information processing in the neostriatum requires elucidation of the processes that control the spatiotemporal pattern of activity of its GABAergic spiny projection neurons, which in rodents make up 90–95% of the neuronal population^{1,2}. Neostriatal spiny projection neurons and the diverse classes of interneurons are interconnected in highly organized synaptic microcircuitry and communicate using numerous neurotransmitters and neuromodulators^{1,2}. Despite the importance of this circuitry, the electrophysiological operation of the neostriatum has so far been understood mostly in terms of the interaction between membrane currents of individual spiny projection neurons and their excitatory corticostriatal input^{2–5}. In contrast, very little is known about the nature and function of intercellular interactions and in particular of fast synaptic signaling among striatal neurons.

GABAergic afferents are major inputs to spiny projection neurons^{6–9} and primary determinants of their activity, as a local pharmacological blockade of GABA_A receptors *in vivo* increases the firing rate of these cells by more than 300% (ref. 10). Furthermore, these inhibitory inputs are behaviorally significant because blockade of GABAergic transmission in the neostriatum results in significant activation and/or disruption of motor behavior^{11,12}. Therefore, GABAergic control of spiny projection neurons may be one of the most powerful determinants of the output of the neostriatum, but its functioning is poorly understood. This is primarily because the identity and physiological properties of the functional afferent sources of GABAergic inputs to spiny projection neurons are not known. Thus we cannot determine the temporal and spatial variability of this input and its dynamic or behavioral contingencies. Largely on the basis of anatomical data¹³, GABAergic inhibition of spiny projection

neurons traditionally has been attributed to lateral inhibition among these cells via their local axon collaterals. Tests of this hypothesis have failed to demonstrate any evidence for lateral inhibition (C.J. Wilson, H. Kita & Y. Kawaguchi, *Soc. Neurosci. Abstr.* 15, 360.1, 1989), and a recent dual recording study¹⁴ has provided compelling evidence that this form of interaction is weak or absent in the neostriatum. These findings led to the alternative hypothesis that certain GABAergic spiny interneurons, which make up only 3–5% of the neurons in the rodent neostriatum, provide the bulk of the inhibitory control of spiny projection cells^{14,15} (C.J. Wilson, H. Kita & Y. Kawaguchi, *Soc. Neurosci. Abstr.* 15, 360.1, 1989).

We examined the synaptic responses of spiny projection neurons to spiking in GABAergic interneurons to test their possible contribution to the strong inhibitory control of the output of the striatum observed *in vivo*. To this end, we adapted recently developed techniques of visualized whole-cell recording^{16–18} to simultaneously record pairs of identified interneurons and projection cells in a mature slice preparation.

RESULTS

Characteristics of interneurons and projection cells

Recorded neurons were identified using primarily physiological and, in some cases, morphological and/or immunocytochemical criteria^{17,19–22}. Spiny projection neurons were readily recognized by their typical membrane properties (Fig. 1a and b). Spiny projection cells (recorded from animals 24–32 days old) were mature as indicated by their membrane properties, including membrane potential (-94.1 ± 1.6 mV, $n = 7$), input resistance (67.4 ± 10.2 M Ω , $n = 8$), inward rectification, action potential threshold (47.3 ± 1.3 mV above rest) and action potential amplitude (80 ± 2.7 mV, $n = 8$), all of which were similar to those observed in slices taken from adults^{17,19–24}. In addition, all intracellularly stained and recovered spiny projection neurons had

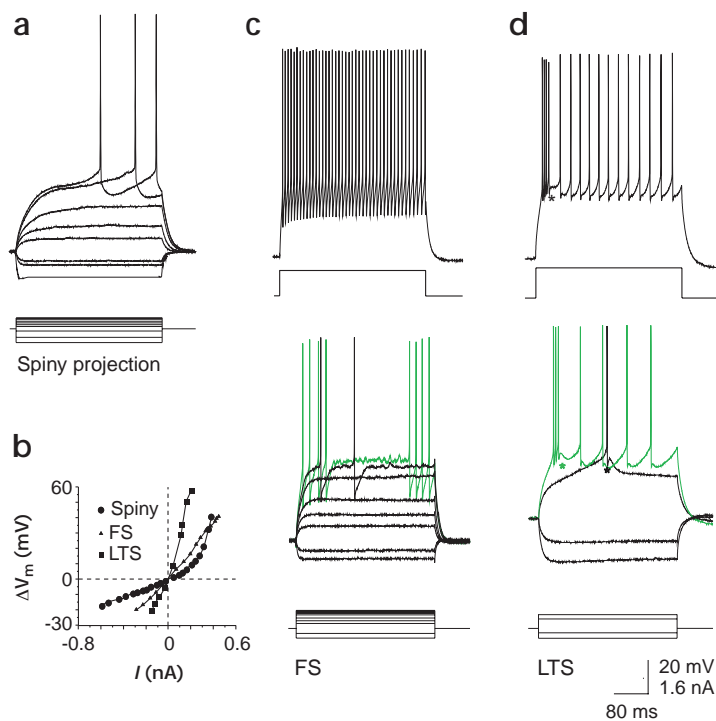


Fig. 1. Characterization of the membrane properties of recorded neurons. **(a)** Spiny projection neurons. Note the strong inward rectification and the depolarizing ramp. **(b)** Differential current–voltage (I – V) relationships of the recorded neuron types. Note the strong inward rectification of spiny projection neurons and the relatively linear I – V curves of the interneurons. **(c)** FS interneurons were characterized by a very high maximal firing frequency (upper panel) and episodic burst firing with subthreshold membrane potential oscillations (green trace) in response to depolarizing current injection. **(d)** LTS interneurons exhibited a regenerative depolarizing ‘hump’ resembling an LTS (asterisks) that always elicited fast spikes. LTS cells had biphasic afterhyperpolarizations. Note the absence of a sustained depolarizing potential (calibration bars apply to a, c and d).

densely spiny dendrites (Fig. 2b), which is a sensitive indicator of their morphological and electrophysiological maturity^{23,24}.

Two physiologically distinct types of interneurons were analyzed. Of the eight interneurons recorded in interacting pairs (a total of eleven pairs), six had the electrophysiological properties of the parvalbumin-containing (PV⁺), fast-spiking (FS) interneurons described previously¹⁷, including narrow action potentials (< 0.5 ms), abruptly peaking, large-amplitude spike afterhyperpolarizations, a relatively linear current–voltage relationship (Fig. 1b) and very high maximal sustained firing frequencies with little or no adaptation (200 ± 23.4 Hz; $n = 5$; Fig. 1c). FS interneurons also showed episodic burst firing and subthreshold membrane potential oscillations (Fig. 1c). FS interneurons were morphologically heterogeneous. Four FS interneurons had morphological characteristics previously reported for PV⁺ FS neurons¹⁷ (Fig. 2a). These neurons were characterized by a soma of

medium to large diameter (16.2 ± 1.6 μ m; range 13–20 μ m; $n = 5$), frequently branching, non-varicose or only slightly varicose aspiny dendrites and a very dense local axon collateral system. The axon collateral arbor overlapped with the dendritic field but tended to extend farther from the soma and covered a oval area with a maximal extent of 388 ± 32 μ m ($n = 3$) and a minimal diameter of 294 ± 39 μ m ($n = 3$). The axon collateral system was more dense in the inner two thirds of the extent of the arborization. Two

other FS neurons had prominent dendritic varicosities and a significantly less dense axonal arbor with larger boutons (Fig. 2b). Two FS interneurons were immunopositive for parvalbumin. These cells belonged to the more common morphological class (data not shown). Their synaptic action could not be tested because of the limit on recording time imposed by the rapid loss of cytoplasmic antigens during whole-cell recording.

Two other interneurons monosynaptically connected to spiny projection cells had electrophysiological properties not previously described in the neostriatum^{17,25}. Their defining feature was the presence of a pronounced regenerative depolarizing potential resembling a low-threshold spike (LTS cells; Fig. 1d). Like FS interneurons, LTS neurons had narrow action potentials and could fire at frequencies up to 300 Hz. However, they had a higher input resistance than FS interneurons (179 ± 114 M Ω , $n = 2$, versus 93.2 ± 26.3 M Ω , $n = 4$; Fig. 1b) and a biphasic spike afterhyper-

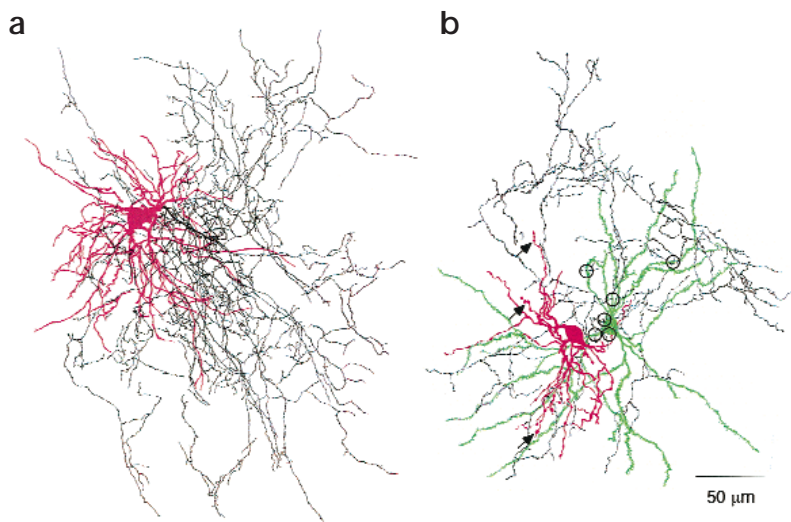


Fig. 2. Camera lucida reconstruction of spiny projection and FS neurons. **(a)** The more common FS interneuron morphology in our sample (dendrites in red, axons in black). These FS interneurons from a 21-day-old animal had aspiny dendrites with little or no varicosities and a dense axonal arborization overlapping with and extending beyond the dendritic field. **(b)** A synaptically connected FS interneuron (red and black) and a spiny projection neuron (green) from a 25-day-old animal. The interneuron is morphologically different from the one shown in **(a)**, exhibiting pronounced dendritic varicosities (arrows), larger axonal boutons and an only moderately dense axonal arbor. The light microscopically identified putative contact sites are perisomatic (circles). The dendrites of the spiny projection cell are densely covered with spines, indicating that the neuron is mature^{23,24}. Axons of the spiny projection neuron are not shown.

polarization. LTS neurons were considered to be different from the persistent depolarization, low-threshold spike (PLTS) interneurons described previously¹⁷ because of the absence of a depolarizing plateau potential (Fig. 1d). Neither of the LTS neurons was recovered, and their morphological and neurochemical identity is unknown. We note however, that the physiological properties of LTS neurons were not very different from PLTS cells, and therefore they may be variants of the same neurochemical cell type. However, neurons showing the distinctive properties of PLTS cells were encountered in our preparation at all ages, which argues against the possibility that LTS neurons of this study differ from previously described PLTS cells simply because of developmental or other differences of the preparations used.

The presence of gap junctions between FS interneurons²⁶ indicates a unique mode of operation for this cell type if these junctions provide significant electrotonic coupling. We tested for significant electrotonic coupling between pairs of FS interneurons. Two of the six pairs of FS interneurons recorded showed evidence of electrotonic coupling (Fig. 3). The coupling ratios were 3% and 20%. This direct demonstration of functional electrotonic coupling among FS interneurons suggests that they may operate in a syncytial fashion.

Biophysical properties of interneuronal IPSPs

FS and LTS neurons provided powerful inhibition to spiny projection neurons within the territory of their axon arbor ($n = 11$ pairs). Approximately 25% of spiny projection neurons recorded within 250 μm from an interneuron showed a synaptic response to activation of the interneuron. The postsynaptic responses elicited from FS and LTS neurons did not differ noticeably with respect to any of the examined properties, and therefore data from the two populations were pooled. Action potentials evoked in the interneurons elicited an inhibitory postsynaptic potential (IPSP; Fig. 4a and b), which was mediated by GABA_A receptors, as it was reversibly blocked by the selective antagonist bicuculline, (20 μM ; $n = 3$; Fig. 4c) and had a reversal potential close to the theoretical equilibrium potential for chloride ions (-74 ± 7.2 mV; $n = 4$; data not shown).

Single presynaptic action potentials evoked variable amplitude IPSPs in the postsynaptic spiny projection neurons. The coefficient of variation of the IPSP amplitude ranged from 0.31 to 1.0. The transmission was very reliable with an average rate of failures of only 0.11 ± 0.06 ($n = 4$). At the resting membrane potential, (approximately -94 mV), the IPSP had an average amplitude of 0.42 ± 0.13 mV, ($n = 5$; range, 0.14 – 0.87 mV). In contrast, the IPSP amplitude was more than twice the resting value (-1.06 ± 0.22 mV; range, -0.33 to -2.13 mV; $n = 7$) when measured at the most depolarized stable membrane potential (7.6 ± 1.8 mV below spike threshold; Fig. 4b). The IPSP also had a longer rise time and a slower decay at this membrane

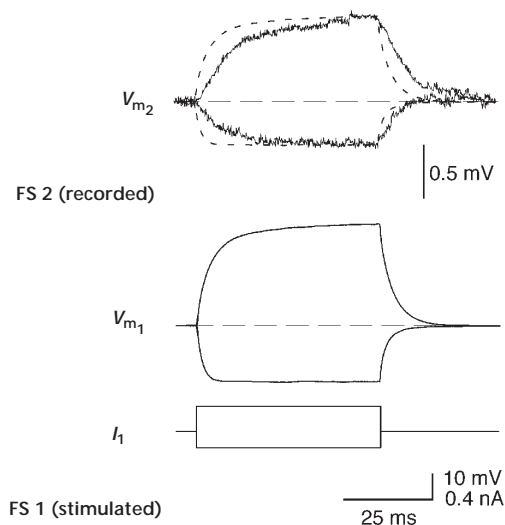


Fig. 3. Electrical coupling between two FS interneurons. Depolarizing or hyperpolarizing current injection into FS 1 (I_1) induces membrane potential deflections in both cells (V_{m1} , V_{m2}). The response is much smaller in FS 2, approximately 3% of that in FS 1. The dashed line in the upper panel (V_{m2}) is the response of FS 1 normalized to the amplitude of the response in FS 1. Note the sigmoid shape of the response of FS 2 due to electrotonic filtering along the dendrites between the two recording sites. (Traces are the average of 20–40 single sweeps).

potential (Fig. 4b). The decay phase of the IPSPs was well fitted with single exponentials in all but one case. The average decay time constant was 15.0 ± 2.3 ms at rest and 36.5 ± 3.5 ms ($n = 3$) at threshold. The larger amplitude (and slower time course) of the IPSP at this membrane potential is due to the higher input resistance (and concomitantly longer time constant) of the spiny projection neurons (Fig. 1a and b), as the driving force of the IPSP is even larger at rest than near threshold.

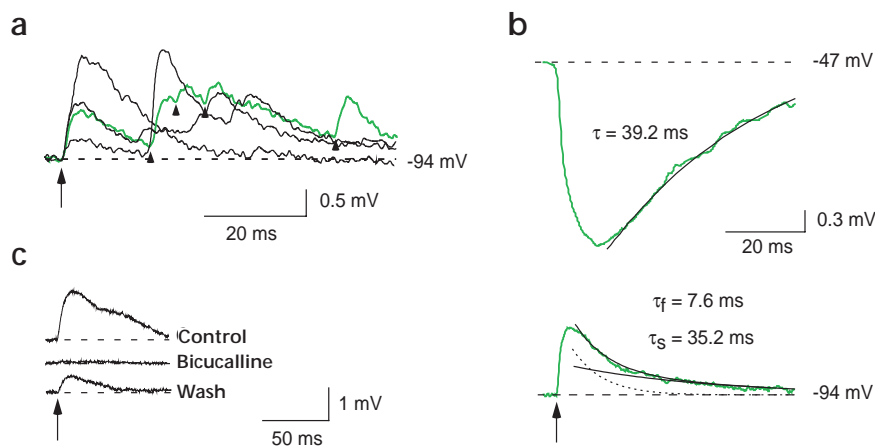


Fig. 4. Properties of IPSPs elicited in spiny projection cells by FS and LTS interneurons. **(a)** Four superimposed sweeps show variable amplitude IPSPs evoked in a spiny projection neuron at rest by an FS interneuron. Presynaptic spikes are indicated by the arrow (stimulated) and arrowheads (spontaneous). **(b)** The amplitude and time course of the IPSP is strongly influenced by the postsynaptic membrane potential. IPSPs evoked by an FS cell in a spiny projection neuron at rest (lower green trace; -94 mV) and near threshold (upper green trace; -47 mV). The IPSP is depolarizing at rest, and it is reversed in sign below threshold. The IPSP amplitude is smaller at rest. **(c)** The IPSP can be reversibly blocked with 20 μM bicuculline applied in the perfusion medium, indicating that it is mediated by GABA_A receptors.

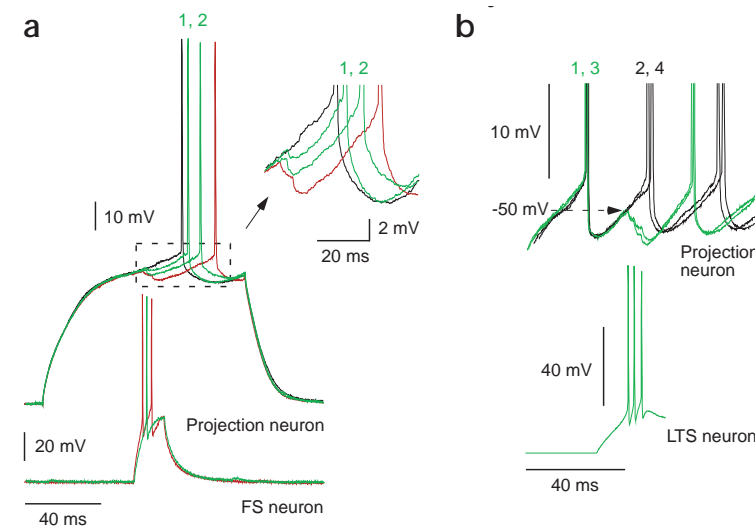


Fig. 5. Interneuronal modulation of action potential generation in spiny projection neurons. **(a)** A single action potential elicited in a spiny projection neuron by current injection (upper black trace) is delayed by IPSPs evoked by single spikes (lower green trace) or a spike doublet (lower red trace) of a FS interneuron. The delay is variable (compare green spikes 1, 2), and the spike doublet (red traces) is more effective than single spikes. The inset shows the IPSPs at higher gain. **(b)** The same experiment as in **(a)** conducted in a pair of an LTS interneurons (lower trace, same cell as in **Fig. 1d**) and a spiny projection cell (upper traces). The LTS of the interneuron elicits three fast spikes (lower trace) evoking compound IPSPs (upper green traces 1, 3) which prevent the firing of the spiny projection cell (black traces 2, 4) for approximately 20 ms. The momentary firing rate is decreased by 35%. The trials were performed in the order of numbering, indicating the stability of the postsynaptic cell and the reliability of the inhibition.

Temporal summation of IPSPs in response to bursts of action potentials in the interneuron (2–5 action potentials occurring within 10–50 ms) resulted in large-amplitude compound responses in spiny projection cells (**Fig. 5a** and **b**). At the most depolarized stable potential, the average amplitude of the compound IPSP was -2.7 ± 0.78 mV (range, -0.8 to -4.6 mV; $n = 5$). Compound IPSPs with significantly larger amplitudes (up to 6–7 mV) could be elicited during spike afterhyperpolarizations of spiny projection neurons made to fire by intracellular depolarizing current injection (**Fig. 5b**).

We tested the cell pairs for the presence of synaptic responses evoked in interneurons by spiny projection neurons under a number of conditions. Single spikes or bursts were elicited in spiny projection neurons while the spike-triggered average of the postsynaptic (interneuronal) membrane potential was recorded at different levels of depolarization. The possibility of both slow (150–1000 ms) and fast responses was investigated, but none was detected, suggesting the absence of a feedback from spiny projection neurons to FS or LTS cells. This observation was supplemented with recordings from eleven additional pairs of synaptically connected FS and spiny projection neurons in slices from younger (16–23 day old) animals.

The upper and lower limits of the number of spiny projection cells innervated by single FS interneurons (divergence) and the number of FS cells synapsing on individual spiny projection neurons (convergence) were estimated based on calculations of the volume of axon arbors of FS interneurons and known striatal cell densities (see Methods). This analysis yielded divergence values of 135–541 spiny projection cells per FS neuron and convergence of 4–27 FS neurons per spiny projection cell.

Interneuronal inhibition of action potential generation

The functional significance of inhibition arising from single interneurons was investigated by examining their influence on the firing of postsynaptic spiny projection neurons. Single or compound IPSPs evoked by FS or LTS interneurons had a profound effect on the generation of action potentials in spiny projection cells. The effect of interneuronal inhibition was tested on spiny projection cells made to fire between 30 and 50 Hz by depolarizing current injection. IPSPs evoked by single presynaptic action potentials in either FS or LTS cells were sufficient to delay the elicited spikes of spiny projection neurons by 5.7 ± 1.4 ms ($n = 4$; range, 3.3–9.4 ms; **Fig. 5a**). IPSP doublets were more effective than single spikes (**Fig. 5a**).

The effect of compound IPSPs elicited by bursts of action potentials in presynaptic interneurons was studied by evoking an LTS-driven burst in LTS neurons or a depolarization-induced burst of 100–200 Hz consisting of 2–5 spikes in FS interneurons. Burst firing in the interneurons was able to cause very long postsynaptic spike delays (24.6 ± 3.8 ms; $n = 6$; range, 10.6–36.3 ms; **Fig. 5b**). Furthermore, the generation of postsynaptic spikes could be blocked reliably by activation of single interneurons if the IPSPs arrived shortly before the expected onset of the firing of the spiny projection cell (**Fig. 5b**). The duration of the delay in the postsynaptic spike correlated with the interspike interval. The delay was shorter at higher postsynaptic firing frequencies and was approximately a constant fraction of the interspike interval. Therefore the inhibitory effect of single interneurons could be expressed as a fractional decrease of momentary firing rate, which was approximately 10% for single and 40% for compound IPSPs.

DISCUSSION

The main finding of the present study is that GABAergic interneurons can exert powerful control on the activity of projection neurons in the neostriatum. The data demonstrate that even single action potentials of one interneuron can significantly decrease the momentary firing rate of its postsynaptic targets. Single FS interneurons are likely to innervate over one hundred spiny projection neurons; therefore the firing of an FS cell will simultaneously block or delay the firing of action potentials in a large population of spiny projection neurons. Furthermore, although our estimates of the convergence and divergence between FS and spiny projection neurons are liable to error, it is likely that each spiny projection neuron is innervated by at least four FS cells. Consequently, inhibition by FS interneurons alone can account for a major fraction of the GABAergic control of spiny projection cells observed *in vivo*. FS as well as other GABAergic interneurons are known to form a feedforward link between the corticostriatal projection and spiny projection cells^{17,25,27,28}. Taken together with the evidence for the absence or weakness of collateral inhibition¹⁴, the strength of the synaptic effect of interneurons indicates that striatal inhibition is primarily or exclusively feedforward. A similar functional organization has been previously inferred from recordings in organotypic cocultures of striatum, cortex and substantia nigra⁴⁸. This conclusion is at variance with many formal

models of neostriatal information processing^{29,30}. The present data suggest a number of additional features of the microcircuitry of neostriatal neurons. First, the lack of inhibition of interneurons by spiny projection cells in our sample of 11 mature and 11 young synaptically connected cell pairs suggest that there is no significant reciprocal feedback from projection neurons to interneurons. Second, there seems to be no inhibition among (FS) interneurons, although our sample of pairs of FS cells tested was very small. Finally, FS interneurons are likely to communicate through electrotonic coupling. The biophysical properties of these various (synaptic or electrotonic) interactions of interneurons may be critical determinants of their population activity, possibly resulting in complex activity patterns^{31,32}.

The present data demonstrate that spiny projection neurons receive strong inhibitory input from at least two physiologically distinct types of interneurons. Because of their different intrinsic membrane properties, FS and LTS neurons are likely to have dissimilar response to synaptic inputs. In particular, the higher input resistance of LTS neurons and their expression of a regenerative depolarizing potential suggest that these neurons may require less strong excitatory input for the firing of action potentials than do FS neurons and that their response may be a short stereotypical burst. Without anatomical and neurochemical identification, the afferents of LTS neurons and their place in the microcircuitry of the neostriatum remain unknown.

Several anatomical features of FS interneurons are inconsistent with a role of providing strictly spatially localized inhibitory input to spiny projection cells. FS interneurons make up only a small fraction (3–5%) of the rodent neostriatal neuronal population^{17,25,26} and have a widely divergent output^{17,25}, each innervating over a hundred spiny projection neurons. Furthermore, we found evidence of electrical coupling in one third of the tested pairs of FS neurons (Fig. 3) which is consistent with previous ultrastructural data. This local syncytial organization suggests a more general regulatory function for neostriatal inhibition. Studies using focal cortical stimulation and immunocytochemical detection of immediate-early gene expression as a measure of striatal activity revealed that FS neurons are indeed activated in wider neostriatal territories, from more extended cortical areas and at a lower threshold than spiny projection cells³³. By integrating the level of activity from a wider cortical area, interneuronal inhibition may suppress the firing of suboptimally excited spiny projection neurons and selectively enable the activation of spiny projection neurons that receive above average cortical excitatory input. In addition, the electrically coupled network of interneurons may synchronously inhibit projection neurons, influencing the temporal relationship of their spike trains^{32,34,35}.

The strong postsynaptic effect and syncytial organization of FS interneurons make them well suited for distributing and amplifying the effects of various striatal afferents, including neuromodulatory inputs. Interneuronal mediation of neuromodulatory control of the functioning of local neuronal circuits has been described in other brain structures such as the cerebral cortex³⁶ or the hippocampus³⁴. It is of particular interest that the dopaminergic and cholinergic control of the firing of spiny projection neurons may in part be mediated by interneuronal inhibition, because PV⁺ interneurons express dopamine receptors³⁷, IPSPs in spiny projection cells are presynaptically inhibited by dopamine^{38,39}, and PV⁺ interneurons receive cholinergic synaptic input from local interneurons⁴⁰. In addition, PV⁺ and NOS⁺ neostriatal GABAergic interneurons may also mediate the effect of other striatal afferents such as the pallidostriatal input⁴¹.

In conclusion, the present data demonstrate that, despite their

small number, neostriatal GABAergic interneurons are powerful determinants of the activity of projection neurons in the neostriatum. This findings potentially open new directions to understanding various normal and pathological processes involving the basal ganglia.

METHODS

Visualized whole-cell recordings were obtained in slices from young adult (24–32 day) and in some cases juvenile (17–21 day) Sprague-Dawley rats. Surgical and other procedures were done with the approval of the Rutgers University Institutional Research Board and in accordance with the NIH Guide to the Care and Use of Laboratory Animals. Eleven synaptically connected pairs of interneurons and spiny projection neurons were recorded in both the older and the younger group (a total of 22 pairs). Older animals were used to ensure the physiological and morphological maturity of recorded neurons and their connections, and all reported physiological data were obtained from the older group. Six of the interneurons from the older group and four from the younger were analyzed morphologically. Pharmacological blockade of the IPSP was demonstrated in slices from the younger group.

Slice preparation. Rats were deeply anesthetized with 80 mg per kg ketamine and 15 mg per kg xylazine i.p., transcardially perfused with 4–5 ml ice-cold modified Ringer's solution (see below) and 300–350 μ m oblique horizontal or coronal sections were cut in the same medium on a Vibroslice (Campden Instruments). The normal Ringer's solution contained 125 mM NaCl, 2.5 mM KCl, 2.5 mM CaCl₂, 1.5 mM MgCl₂, 26 mM NaHCO₃, 1.25 mM NaH₂P0₄ and 9 mM glucose (pH 7.3–7.4). In the modified solution, NaCl was substituted for choline chloride, and the solution contained 0.3 mM CaCl₂ and 3.7 mM MgCl₂. Slices were incubated in normal Ringer's solution at 31–33° for 1–2 h immediately after sectioning.

Visualized whole-cell recording. Recordings were obtained with borosilicate pipettes pulled from 1.5 diameter tubing (W.P.I.) having 5–8 M Ω impedances. The intracellular solution contained 129.4 mM K-gluconate, 11.1 mM KCl, 2 mM MgCl₂, 10 mM HEPES, 3 mM Na₂ATP, 0.3 mM GTP and 0.02 mM EGTA (pH 7.2–7.3). E_{Cl}⁻ = -58 mV at 35°C. The equilibrium potential for chloride was set at -58 mV based on reversal potential measurements of GABA_A responses in spiny projection cells^{23,42}. Membrane potential measurements were corrected for the liquid junction potential off line by 8 mV calculated from the generalized Henderson equation^{43,44}. Recordings were made with a Neurodata IR-283 dual channel current clamp amplifier. Neurons were visualized under infrared differential interference contrast (IR-DIC) microscopy using an Olympus BX50 microscope equipped with a 40 \times long-working-distance water immersion objective. Interneurons were targeted based on their differential appearance under IR-DIC. For neurotransmitter/receptor identification, 20 μ M bicuculline methochloride (Sigma) was applied in the superfusion medium.

Histological procedures. Interneurons and spiny projection neurons were recorded with micropipet filled with the intracellular solution containing 0.6% and 0.15% biocytin, respectively. Visualization of biocytin and double-labeling immunocytochemistry were done with modifications of described procedures^{17,45}. Briefly, slices were immersion fixed in 4% paraformaldehyde and 0.3% picric acid for 1–4 h at RT and resectioned at 50 or 60 μ m. Sections were then incubated in 1% NaBH for 50 minutes and in a mixture of 3% H₂O₂ and 10% methanol for 15 minutes. For visualization of biocytin alone, sections were incubated in PB containing 0.5% Triton X-100 and 1:200 ABC reagent (Vector) overnight and reacted with 3,3'-diaminobenzidine as a chromogen (in most cases using nickel intensification). For double-labeling immunocytochemistry, sections were incubated overnight in PB containing 2% bovine serum albumin, 10% normal goat serum, 0.5% Triton X-100 and a mouse monoclonal α -PV IgG (Sigma) at 1:2000 dilution. Biocytin was then visualized by incubation in 1:300 AMCA conjugated streptavidin (Jakson Laboratories) and parvalbumin was visualized with 1:600 Cy3 conjugated goat α -mouse IgG (Sigma). The neurons were examined using an Olympus BX60 epifluorescence microscope with standard filter sets. Neurons were reconstructed on a Nikon Optiphot microscope under a 100 \times -oil immersion objective using a drawing tube.

Data analysis. Convergence and divergence values were estimated on the basis of the volume of the axon arbor of FS cells and the density of spiny projection neurons. The average volume of the axon arbor of FS neurons was $6.85 \pm 1.19 \times 10^{-3} \text{ mm}^3$ ($n = 4$) in our sample, assuming a three-dimensionally symmetrical axon arbor. The neuron density in the striatum is 84,900 cells per mm^3 (refs. 46, 47), which corresponds to 541 ± 101 spiny projection neurons within the axon arbor of an FS cell, the upper limit of divergence. The upper limit of convergence is 27 FS cells per spiny projection neuron if all spiny projection neurons are innervated within the presynaptic axon arbor and if FS cells make up their estimated maximal population of 5% (refs. 25, 26). As approximately one quarter of the spiny projection neurons show synaptic interaction in the vicinity of an FS cell (within 250 μm), a minimal divergence of 135 spiny projection neurons per FS cell and convergence of 4 FS neurons per spiny projection cell can be calculated for the minimal FS neuron population of 3% (refs. 25, 26).

ACKNOWLEDGEMENTS

We thank K. Moore and K. Pang for help during the early phase of this experiments, J.P. Bolam, A. Sik and L. Záborszky for advice concerning anatomical methods, G. Buzsáki, A. Czurkó, A. Göndöcs, C. Paladini and D. Shohamy for critically reviewing the manuscript and F. Shah for technical assistance. Supported by MH58885, NS34865 and Rutgers University Busch-BRSO funds.

RECEIVED 19 JANUARY; ACCEPTED 11 MARCH 1999

1. Bolam, J. P. & Bennett, B. D. in *Molecular and Cellular Mechanisms of Neostriatal Function* (eds. Marjorie, A., Ariano, M. A. & Surmeier, D. J.) 1–2 (Springer, Heidelberg, 1993).
2. Gerfen, C. R. & Wilson, C. J. in *Handbook of Chemical Neuroanatomy* Vol. 12 *Integrated Systems of the CNS* (eds. Swanson, L. W., Björklund, A. & Hökfelt, T.) 371–468 (Elsevier Science B.V., Amsterdam, 1996).
3. Wilson, C. J. & Kawaguchi, Y. The origins of two-state spontaneous membrane potential fluctuations of neostriatal spiny neurons. *J. Neurosci.* **16**, 2397–2410 (1996).
4. Wilson, C. J., Chang, H. T. & Kitai, S. T. Origins of post synaptic potentials evoked in spiny neostriatal projection neurons by thalamic stimulation in the rat. *Exp. Brain Res.* **51**, 217–226 (1983).
5. Wilson, C. J. in *Single Neuron Computation* (eds. McKenna, T., Davis, J. & Zornetzer, S. F.) 141–171 (Academic, San Diego, 1992).
6. Lighthall, J. W., Park, M. R. & Kitai, S. T. Inhibition in slices of rat neostriatum. *Brain Res.* **212**, 182–187 (1981).
7. Lighthall, J. W. & Kitai, S. T. A short duration GABAergic inhibition in identified neostriatal medium spiny neurons: *in vitro* slice study. *Brain Res. Bull.* **11**, 103–110 (1983).
8. Calabresi, P., Mercuri, N. B., Stefani, A. & Bernardi, G. Synaptic and intrinsic control of membrane excitability of neostriatal neurons. I. An *in vivo* analysis. *J. Neurophysiol.* **63**, 651–662 (1990).
9. Kita, H. Glutamatergic and GABAergic postsynaptic responses of striatal spiny neurons to intrastriatal and cortical stimulation recorded in slice preparations. *Neuroscience* **70**, 925–940 (1996).
10. Nisenbaum, E. S. & Berger, T. W. Functionally distinct subpopulations of striatal neurons are differentially regulated by GABAergic and dopaminergic inputs—I. *In vivo* analysis. *Neuroscience* **48**, 561–578 (1992).
11. Yoshida, M., Nagatsuka, Y., Muramatsu, S. & Nijima, K. Differential roles of the caudate nucleus and putamen in motor behavior of the cat as investigated by local injection of GABA antagonists. *Neurosci. Res.* **10**, 34–51 (1991).
12. Yamada, H., Fujimoto, K. & Yoshida, M. Neuronal mechanism underlying dystonia induced by bicuculline injection into the putamen of the cat. *Brain Res.* **677**, 333–336 (1995).
13. Wilson, C. J. & Groves, P. M. Fine structure and synaptic connections of the common spiny neuron of the rat neostriatum: a study employing intracellular injection of horseradish peroxidase. *J. Comp. Neurol.* **194**, 599–615 (1980).
14. Jaeger, D., Kita, H. & Wilson, C. J. Surround inhibition among projection neurons is weak or nonexistent in the rat neostriatum. *J. Neurophysiol.* **72**, 1–4 (1994).
15. Kita, H. GABAergic circuits of the striatum. *Prog. Brain Res.* **99**, 51–72 (1993).
16. Dödt, H. U. & Zieglerberger, W. Visualizing unstained neurons in living brain slices by infrared DIC—videomicroscopy. *Brain Res.* **537**, 333–336 (1990).
17. Kawaguchi, Y. Physiological, morphological, and histochemical characterization of three classes of interneurons in rat neostriatum. *J. Neurosci.* **13**, 4908–4923 (1993).
18. Miles, R. & Poncer, J. C. Paired recordings from neurones. *Curr. Opin. Neurobiol.* **6**, 387–394 (1996).
19. Kita, T., Kita, H. & Kitai, S. T. Passive electrical membrane properties of rat neostriatal neurons in an *in vitro* slice preparation. *Brain Res.* **300**, 129–139 (1984).

20. Kita, H., Kita, T. & Kitai, S. T. Active membrane properties of rat neostriatal neurons in an *in vitro* slice preparation. *Exp. Brain Res.* **60**, 54–62 (1985).
21. Kawaguchi, Y., Wilson, C. J. & Emson, P. C. Intracellular recording of identified neostriatal patch and matrix spiny cells in a slice preparation preserving cortical inputs. *J. Neurophysiol.* **62**, 1052–1068 (1989).
22. Nisenbaum, E. S., Xu, Z. C. & Wilson, C. J. Contribution of a slowly inactivating potassium current to the transition to firing of neostriatal spiny projection neurons. *J. Neurophysiol.* **71**, 1174–1189 (1994).
23. Tepper, J. M. & Trent, F. *In vivo* studies of the postnatal development of rat neostriatal neurons. *Prog. Brain Res.* **99**, 35–50 (1993).
24. Tepper, J. M., Sharpe, N. A., Koós, T. Z. & Trent, F. Postnatal development of the rat neostriatum: electrophysiological, light- and electron-microscopic studies. *Dev. Neurosci.* **20**, 125–145 (1998).
25. Kawaguchi, Y., Wilson, C. J., Augood, S. J. & Emson, P. C. Striatal interneurons: chemical, physiological and morphological characterization. *Trends Neurosci.* **18**, 527–535 (1995).
26. Kita, H., Kosaka, T. & Heizmann, C. W. Parvalbumin-immunoreactive neurons in the rat neostriatum: a light and electron microscopic study. *Brain Res.* **536**, 1–15 (1990).
27. Bennett, B. D. & Bolam, J. P. Synaptic input and output of parvalbumin immunoreactive neurons in the neostriatum of the rat. *Neuroscience* **62**, 707–719 (1994).
28. Kawaguchi, Y. & Kubota, Y. GABAergic cell subtypes and their synaptic connections in rat frontal cortex. *Cereb. Cortex* **7**, 476–486 (1997).
29. Wickens, J. R., Köster, R. & Alexander, M. E. Effects of local connectivity on striatal function: stimulation and analysis of a model. *Synapse* **20**, 281–298 (1995).
30. Groves, P. M. A theory of the functional organization of the neostriatum and the neostriatal control of voluntary movement. *Brain Res.* **286**, 109–132 (1983).
31. Rinzel, J., Terman, D., Wang, X. & Ermentrout, B. Propagating activity patterns in large-scale inhibitory neuronal networks. *Science* **279**, 1351–1355 (1998).
32. Whittington, M. A., Traub, R. D. & Jefferys, J. G. Synchronized oscillations in interneuron networks driven by metabotropic glutamate receptor activation. *Nature* **373**, 612–615 (1995).
33. Parthasarathy, H. B. & Graybiel, A. M. Cortically driven immediate-early gene expression reflects modular influence of sensorimotor cortex on identified striatal neurons in the squirrel monkey. *J. Neurosci.* **17**, 2477–2491 (1997).
34. Freund, T. F. & Buzsáki, G. Interneurons of the hippocampus. *Hippocampus* **6**, 347–470 (1996).
35. Cobb, S. R., Buhl, E. H., Halasy, K., Paulsen, O. & Somogyi, P. Synchronization of neuronal activity in hippocampus by individual GABAergic interneurons. *Nature* **378**, 75–78 (1995).
36. Xiang, Z., Huguenard, J. R. & Prince, D. A. Cholinergic switching within neocortical inhibitory networks. *Science* **281**, 985–988 (1998).
37. Lenz, S., Perney, T. M., Qin, Y., Robbins, E. & Chesselet, M. F. GABA-ergic interneurons of the striatum express the Shaw-like potassium channel, Kv3.1. *Synapse* **18**, 55–66 (1994).
38. Nicola, S. M. & Malenka, R. C. Dopamine depresses excitatory and inhibitory synaptic transmission by distinct mechanisms in the nucleus accumbens. *J. Neurosci.* **17**, 5697–5710 (1997).
39. Pennartz, C. M. A., Dolleman-Van Der Weel, M. J., Kitai, S. T. & Da Silva, F. H. L. Presynaptic dopamine D1 receptors attenuate excitatory and inhibitory limbic inputs to the shell region of the rat nucleus accumbens studied *in vitro*. *J. Neurophysiol.* **67**, 1325–1334 (1992).
40. Chang, H. T. & Kita, H. Interneurons in the rat striatum: relationships between parvalbumin neurons and cholinergic neurons. *Brain Res.* **574**, 307–311 (1992).
41. Bevan, M. D., Booth, P. A. C., Eaton, S. A. & Bolam, J. P. Selective innervation of neostriatal interneurons by a subclass of neuron in the globus pallidus of the rat. *J. Neurosci.* **18**, 9438–9452 (1998).
42. Jiang, Z. G. & North, R. A. Membrane properties and synaptic responses of rat striatal neurones *in vitro*. *J. Physiol. (Lond.)* **443**, 533–553 (1991).
43. Barry, P. H. JPCalc, a software package for calculating liquid junction potential corrections in patch-clamp, intracellular, epithelial and bilayer measurements and for correcting junction potential measurements. *J. Neurosci. Methods* **51**, 107–116 (1994).
44. Ng, B. & Barry, P. H. The measurement of ionic conductivities and mobilities of certain less common organic ions needed for junction potential corrections in electrophysiology. *J. Neurosci. Methods* **56**, 37–41 (1995).
45. Horikawa, K. & Armstrong, W. E. A versatile means of intracellular labeling: injection of biocytin and its detection with avidin conjugates. *J. Neurosci. Methods* **25**, 1–11 (1988).
46. Oorschot, D. E. Total number of neurons in the neostriatal, pallidal, subthalamic, and substantia nigra nuclei of the rat basal ganglia: A stereological study using the cavalieri and optical disector methods. *J. Comp. Neurol.* **366**, 580–599 (1996).
47. Kincaid, A. E., Zheng, T. & Wilson, C. J. Connectivity and convergence of single corticostriatal axons. *J. Neurosci.* **18**, 4722–4731 (1998).
48. Plenz, D. & Kitai, S. T. Up and down states in striatal medium spiny neurons simultaneously recorded with spontaneous activity in fast-spiking interneurons studied in cortex-striatum-substantia nigra organotypic cultures. *J. Neurosci.* **18**, 266–283 (1998).